UDC 621.039.54

# DISPERSION FUEL FOR NUCLEAR RESEARCH FACILITIES

*A.V. Kushtym, M.M. Belash, V.V. Zigunov, O.O. Slabospitska, V.A. Zuyok*
*"Nuclear Fuel Cycle" Science and Technology Establishment*
*National Science Center "Kharkov Institute of Physics and Technology", Kharkov, Ukraine*
*E-mail: kushtym@kipt.kharkov.ua*

Designs and process flow sheets for production of nuclear fuel rod elements and assemblies TVS-XD with dispersion composition $UO_2$+Al are presented. The results of fuel rod thermal calculation applied to Kharkiv subcritical assembly and Kyiv research reactor VVR-M, comparative characteristics of these fuel elements, the results of metallographic analyses and corrosion tests of fuel pellets are given in this paper.

## INTRODUCTION

Developed fuel assemblies TVS-XD with fuel rod elements and $UO_2$+Al fuel element kernel can be utilised within a nuclear facilites «Neutron source based on subcritical assembly (SCA) controlled by an electron accelerator» and research swimming pool reactor VVR-M [1–3]. Fuel assemblies have been designed as compatible and replaceable ones with currently utilised FA VVR-M2 for possibility of their complete or partial replacement in the active core of nuclear facilites.

While developing fuel element and fuel assembly designs evaluation of their temperatures with the aid of thermomechanical code TRANSURANUS has been performed [4].

The purpose of this paper is to develop fuel assembly designs, fuel element model and fuel pellet production operations, execution of their metallographic analyses and corrosion testing, calculation of temperature fields in fuel elements.

## 1. DESIGNS OF FUEL ROD ASSEMBLIES

Fuel rod assemblies (FRA) TVS-XD are similar in their dimensions and isotope $U^{235}$ content to FRA VVR-M2 [5–7]. Their design features are presence of a rigid welded framework and providing possibilities for convenient assembly and bonding fuel elements within it. TVS-XD1 and TVS-XD2 comprised of 6 and 18 fuel elements, respectively, with claddings of E110 or E-635 alloys and pellets of dispersion compositions of uranium dioxide in the form of kernels or spheres dispersed in the matrix of aluminium alloy.

The process of fuel element model production includes the following process stages: encapsulation of the lower blind joint with cladding by electric-arc welding, filling the cladding with pellets, setting-up the holder, filling the cladding with helium and its encapsulation with the upper blind joint.

The design of fuel element of linked type, in which dispersion core piece metallurgic ally coupled with its cladding offers promise for the industry. As materials for cladding both zirconium-base alloys (E110, E-635) and aluminium alloys like CAB-1, CAB-6, AMCH-2, AMg2, 6061 etc. can be applied [8].

The structure of TVS-XD1 (Fig. 1) is comprised of the following: upper and lower spacer grids, central tube, connection unit, upper end piece, muft, bottom nozzle and fuel elements.

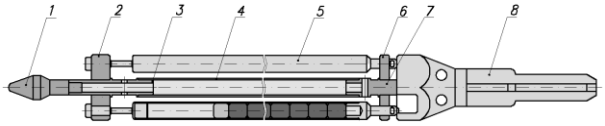


*Fig. 1. Design of TVS-XD1 [1]: 1 – head; 2 – upper grid; 3 – connector adapter; 4 – central tube; 5 – dispersion nuclear fuel element; 6 – lower grid; 7 – muft; 8 – bottom nozzle*

In the structure of TVS-XD2 (Fig. 2) the outer diameter of fuel elements was decreased and their number was increased from 6 up to 18 [2]. Their cladding was made of E110 alloy, and dispersion fuel composition is in the form of pellets containing $UO_2$+Al.

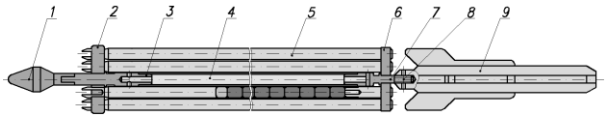


*Fig. 2. Design of TVS-XD2 [2]: 1 – head; 2 – upper grid; 3 – connector adapter; 4 – central tube; 5 – dispersion nuclear fuel element; 6 – lower grid; 7 – muft; 8 – connection unit; 9 – bottom nozzle*

The appearance of manufactured models of TVS-XD1, fuel elements and fuel pellets are given on Fig. 3, and specific design features of spacer grids are given on Fig. 4.

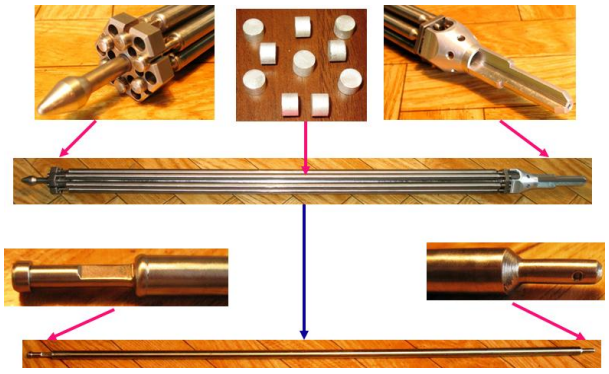

*Fig. 3. Fuel element and TVS-XD1 models*

Operating conditions of FRA VVR-M2 and TVS-XD in the active cores of SCA and VVR-M are given in Tabl. 1, and their design, estimated and comparative characteristics are given in Tables 2, 3, and 4, respectively.

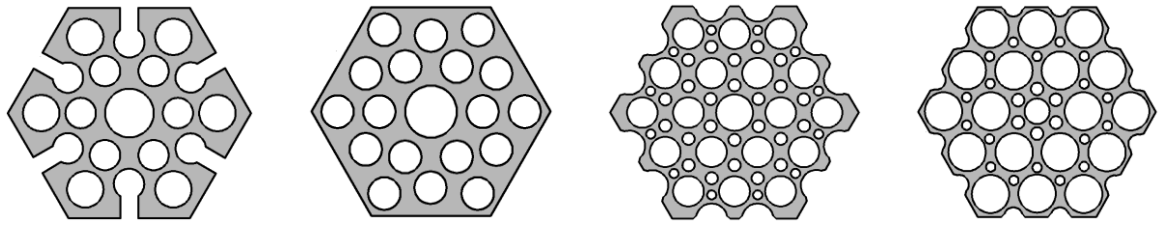

*a* *b* *c* *d*

*Fig. 4. Designs of spacer grids of TVS-XD1 (a – the upper one, b – the lower one) and TVS-XD2 (c – the upper one, d – the lower one)*

Table 1

Operating conditions of FRA VVR-M2 and TVS-XD in the active cores of SCA and VVR-M

| Characteristics | SCA | VVR-M |
|---|---|---|
| Thermal power, MW | 0.26 | 10 |
| Number of fuel assemblies/fuel elements in the active core (XD1/XD2) | 36/(216/648) | 262/(1572/4716) |
| Coolant temperature at the outlet of active core, $^{o}$C | ≤40 | 50...65 |
| Upper design temperature of fuel element cladding, $^{o}$C | ≤99 | ≤99 |
| Coolant saturation temperature, $^{o}$C | 103 | 102…103 |
| Onset temperature of surface boiling on the cladding, $^{o}$C | 115 | 115 |

Table 2

Design characteristics of TVS-XD

| Characteristics | TVS-XD1 | TVS-XD2 |
|---|---|---|
| "Turn key" fuel assembly dimension, mm | 35 | 35 |
| Number of fuel elements in fuel assembly | 6 | 18 |
| Outer diameter of fuel-element cladding, mm | 9.1 | 5.85 |
| Inner diameter of fuel-element cladding, mm | 7.72 | 4.75 |
| Fuel pellet diameter, mm | 7.57 | 4.6 |
| Thermal column height, mm | 500 | 500 |
| Fuel element grid spacing in fuel assembly, mm | 12.75 | 7.90 |
| Isotope $^{235}$U enrichment, % | 19.75 | 19.75 |
| Weight of $^{235}$U, g | 50 | 50 |
| Weight of uranium ($^{235}$U + $^{238}$U), g | 250 | 250 |
| Volumetric fraction of $UO_2$ particles in the matrix, % | 20.5 | 20.5 |

Table 3

Some of calculated characteristics of TVS-XD of various designs with $UO_2$+Al composition

| Characteristics | TVS-XD1 | TVS-XD2 |
|---|---|---|
| Heat-transfer surface area, cm$^2$ | 857.66 | 1654.05 |
| Fuel assembly clear area, cm$^2$ | 6.68 | 5.75 |
| Hydraulic diameter, mm | 15.58 | 6.95 |
| Specific surface area per unit volume of the active core, cm$^2$/cm$^3$ | 1.62 | 3.12 |
| $UO_2$+Al fuel composition volume, cm$^3$ | 135.02 | 149.57 |
| $UO_2$+Al fuel composition weight, g | 283.7 | 283.7 |
| Fuel composition density, g/cm$^3$ | 4.26 | 4.10 |

Table 4

Comparative characteristics of basic FRA VVR-M2 and engineered TVS-XD

| Characteristics | FA VVR-M2 | TVS-XD1 | TVS-XD2 |
|---|---|---|---|
| Fuel composition volume, cm$^3$ | 95.08 | 135.02 | 149.57 |
| Energy conduction surface, m$^2$ | 0.190 | 0.086 | 0.165 |
| Specific surface area per unit volume of the active core, cm$^2$/cm$^3$ | 3.585 | 1.617 | 3.120 |
| Clear area, cm$^2$ | 5.85 | 6.68 | 5.75 |
| Hydraulic diameter, mm | 5.00 | 15.60 | 6.92 |
| Fuel-water ratio | 0.325 | 0.404 | 0.797 |

## 2. TEMPERATURE EVALUATION IN FUEL ELEMENTS

In order to determine operability of fuel elements an evaluation of their temperatures and thermal stresses is required. The group of thermophysical criteria limits maximum temperatures of fuel composition, the cladding of fuel element and its maximum linear heat generation rate [7].

In the first option, temperature in the fuel elements were evaluated using the known numerical dependencies, and in the second option, the calculation was performed using a modified TRANSURANUS code model for dispersion fuel. After the calculations their results were compared and determined calculation errors.

To determine the operating temperature of the fuel core piece with conservative approach thermal gradients within the cladding, the gap and along the pellet radius were calculated, and made allowance for thermal conductivity coefficients of the dispersion composition and the matrix (Fig. 5).

Variation in thermal conductivity of helium filling the internal volume of fuel element depending on fuel burn-up has been taken into consideration since due to generation of gaseous fission products within the gap helium thermal conductivity decreases that increases temperature gradient between the cladding and fuel core piece.

The thermal conductivity coefficient of dispersion fuel compositions is determined with some level of approximation according to Odelevskiy's formula [8]:

$$\lambda_{comp} = [(3V_M - 1)\cdot\lambda_M + (3V_T - 1)\cdot\lambda_T]/4 + \\ + \sqrt{[(3V_M - 1)\cdot\lambda_M + (3V_T - 1)\cdot\lambda_T]^2/16 + (\lambda_M \cdot \lambda_T)/2}\ , \quad (1)$$

where $\lambda_M$ is the thermal conductivity coefficient of matrix material; $\lambda_T$ is the thermal conductivity coefficient of fuel material; $V_T$ is the volumetric fraction of fuel material; $V_M$ is the volumetric volume of matrix material.

The calculation results show that presence of gas gap significantly increases the temperature of dispersion fuel composition while the coupled version of the fuel element is operable at higher thermal loads.

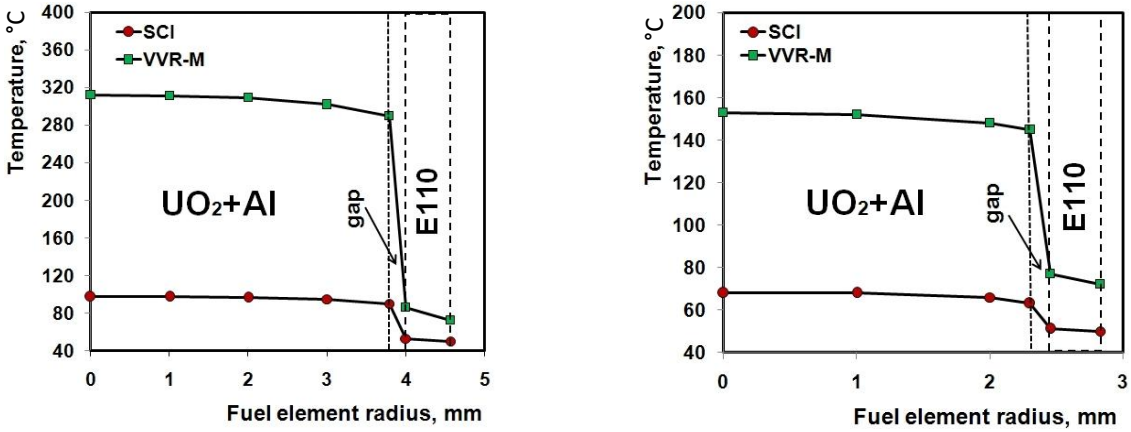


*Fig. 5. Fuel element radial temperature distribution at a designed capacity of SCA (260 kW) and VVR-M (10000 kW): a – TVS-XD1 (fuel elements Ø 9.1 mm); b – TVS-XD2 (fuel elements Ø 5.85 mm)*

In the first option, the maximum temperatures of the kernels of fuel elements TVS-XD1 and TVS-XD2 constituted for SCA ~ 95 and ~ 70 °C, and for VVR-M ~ 315 and ~ 155 °C, respectively.

The calculation of fuel element temperatures for different heat flow with the aid of TRANSURANUS code showed that temperatures in the centre of the fuel kernel in the fuel element of container type TVS-XD1 amounted for SCA ~ 85 °C, and for VVR-M reactor ~ 250 °C. For fuel element of coupled type temperature for SCA amounted to ~ 50 °C, and for VVR-M reactor ~ 65 °C.

Also, in temperature calculations the volume of fuel reacted with a matrix, which degrade the thermal conductivity of the fuel composition and increase temperature in the particles of uranium dioxide, should be taken into account [8]. Thus, the temperature of dispersion composition of uranium dioxide in aluminium matrix is within acceptable limits (taking into account the error of calculation of ±(5...7)%).

## 3. DISPERSION COMPOSITIONS OF $UO_2$+Al

### 3.1. A MATRIX OF ALUMINIUM ALLOY

Applied aluminum alloy powders (Tabl. 5) had shapes close to plate-like one. Determination of their physico-technological properties were performed in compliance with the following methods: particle size distribution according to GOST 18318-94, particle shape according to GOST 25849-83, bulk density according to GOST 19440-94 and compactibility according to GOST 25280-90.

The study of compactibility of aluminium alloy powders were carried out on fractions of: 50...112; 112...315; 500...700, and 800...1000 μm. Mechanical classification was conducted by dry powder sieve analysis. The powder molding (Fig. 6) in the work-pieces were executed in a steel cylindrical mold with two punches changing compression compacting pressure in the range of 300...800 MPa. Polyethylene glycol was used as a binder.

*a* *b* *c* *d*

*Fig. 6. Appearances of aluminium alloy powder fractions: a – 50…112; b – 112…315; c – 500…700; d – 800…1000 μm*

Table 5

Chemical composition (% weight) of aluminium powders employed

| Alloying addition → | Mg | Si | Cu | Cr | Fe | The basis |
|---|---|---|---|---|---|---|
| AP (GOST 6058-73) | – | 0.4 | 0.02 | – | 0.5…0.8 | Al |
| Aluminium alloy | 0.8…1.2 | 0.4…0.8 | 0.35…0.65 | 0.03…0.1 | – | Al |

Production of pellets of aluminum alloy powders was carried out according to a two-stage cold compression, which included basic operations: dosing of powders, mixing with the binder, cold compression of workpieces, vacuum annealing, cold deformation in the mold of larger diameter, sintering in vacuum at the temperature range of 450...640 °C.

As can be seen from Fig. 7, in the pressure range of 300...600 MPa the relative density of work pieces increased linearly, and with further increase in pressure the values of relative density varied slightly.

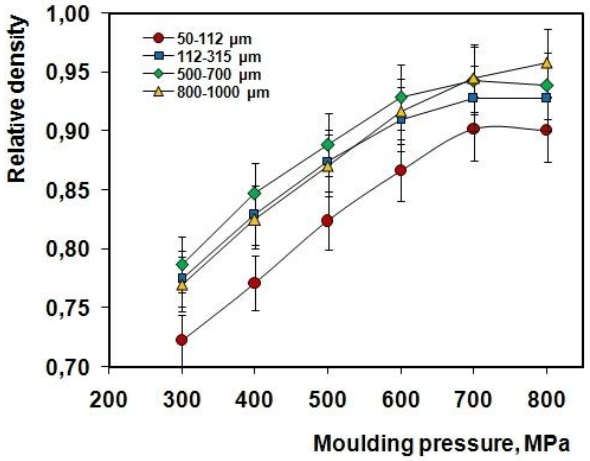


*Fig. 7. Relative density of work pieces depending on specific moulding pressure and particle grain size of aluminium alloy powder*

Relative density of pellets was determined at different stages of production by the methods of hydrostatic weighing and measuring in the air.

With increase in size of the powders a tendency to an increase in the values of relative density of workpieces was traced. On the straight-line portion workpiece compacting was pretty exactly governed by M.Yu. Balshin's equation [9]:

$$\lg P = m \lg \rho + \lg P_{\max}, \qquad (2)$$

where $\rho$ is the relative density of work-piece, %; $P$ is the specific strength moulding, MPa; $P_{\max}$ is the specific strength moulding, which required for obtaining a work-piece of 100% solidness; $m$ is a moulding factor.

Graph plotting in logarithmic coordinates allows determining the values of factor m and specific strength, $P_{\max}$, which is equal to the tangent of the angle of inclination of straight line to axis $\lg\rho$ and an interval intercepted by this line on $\lg P$ axis, respectively.

The values of factor m is constant and independent of the particle size distribution of the starting powders and their bulk density equal to the value of 4.1±0.1 for all cases. The values of $P_{\max}$ depend on mentioned parameters and decrease with increasing particle size of the powder from 1047 to 816...860 MPa.

After pressing the work-pieces of aluminium alloy powders, in order to relieve stress and to strip the binder annealing in a vacuum furnace at 620 °C was conducted, which resulted in some increase in the specific gravity of work-pieces (up to 2%).

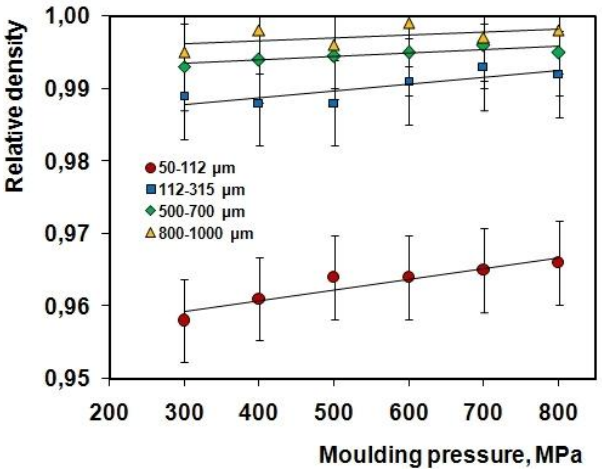


*Fig. 8. Relative density of work pieces of aluminium alloy powder depending on moulding pressure and their grain particle size after vacuum annealing at 620 ℃, repeated cold deformation at 800 MPa and sintering at 620 ℃ in vacuum*

After repeated cold deformation and sintering in vacuum the pellets produced of aluminium alloy powders of fine fraction 50…112 μm have porosity between 5 and 7%. Repeated deformation of work pieces in the cylindrical press mould of higher diameter (0.6 mm more) under the specific pressure of 800 MPa and the following annealing at 620 °C in vacuum for 2 hours ensures relative density of pellets produced of three higher fractions

of aluminium powder (except fraction 50…112 μm) about 99% of the theoretical value (Fig. 8). Powders of fraction 112…315 μm had good compactibility, the effect of pre-annealing temperature on final porosity of pellets from this fraction was insignificant, minimum porosity of samples was ~ 1%.

The results of metallographic analyses of pellets formed from different fractions of aluminium alloy powder are shown in Fig. 9.

In thin sections of pellets produced of the fine fraction of 50...112 μm a layered structure of the matrix with the grain size of 5...7 μm and a shape preferably pulled in one direction were observed. Their pore size was 10…12 μm, pores of irregular shape were observed, the nature of their distribution was uneven. These pores could form chains with size up to 45...50 μm and were observed in the intergranular zone and on powder particle contact boundaries. Matrix microhardness was 432…525 MPa.

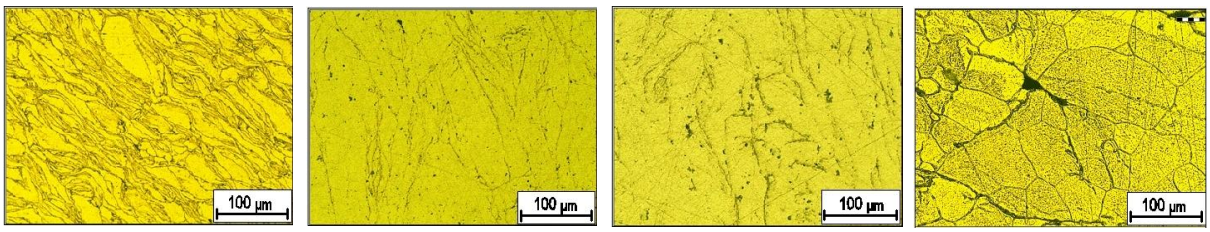


*a* *b* *c* *d*

*Fig. 9. Microstructure of matrix moulded of aluminium alloy powder: a – 50…112; b – 112…315; c – 500…700; d – 800…1000 μm*

### 3.2. PRODUCING FUEL PARTICLES OF $UO_2$

As the fuel component of dispersion composition $UO_2$+Al uranium dioxide powder (TU 95.213-73) was used. It was utilized for production of sintered particles in the form of kernels and the microspheres of specified fractional composition (Tabl. 6) by the methods of powder metallurgy.

Kernels was obtained by crushing pressed and sintered pellets of $UO_2$ powder. Kernels was irregular in its shape (comminuted). When obtaining microspheres the spheroidizing of semifinished cylindrical work-pieces was carried out with a spheronizer. The appearance of particles of uranium dioxide is shown in Fig. 10.

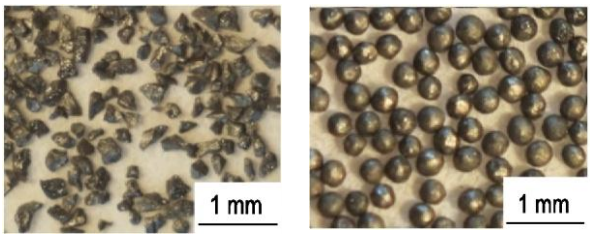


*a* *b*

*Fig. 10. Appearance of $UO_2$ fuel particles: a – kernels; b – spheres*

Table 6

Characteristics of uranium dioxide particles

| Particle shape | Size, μm | Density, g/cm$^3$ | Method for obtaining |
|---|---|---|---|
| Spheres | 200…400 | 9.0…9.8 | spheroidizing semi-finished work-pieces |
| Kernels | | 10.4 | pellet crushing |

### 3.3. PELLETIZING $UO_2$+Al

Process stages of producing pellets containing $UO_2$+Al were brought into effect according to the flow diagram exhibited in Fig. 11 in the following sequence: preparing a mixture of aluminium alloy powder and granulated particles of $UO_2$, adding a binder, mixing press charge, drying, press forming cylindrical work pieces, vacuum annealing, repeated cold deformation of work-pieces, pellet sintering in vacuum furnace.

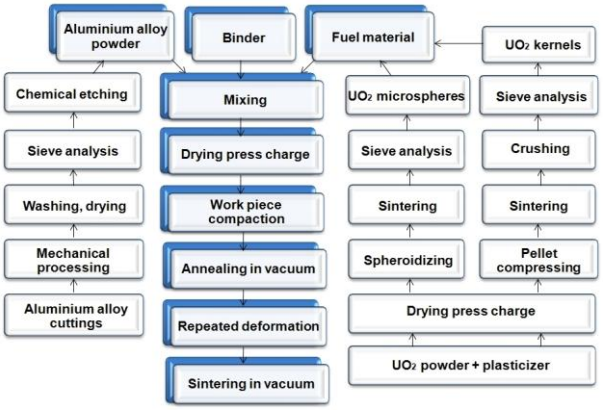


*Fig. 11. Process flow sheet of $UO_2$+Al fuel pellet production [3]*

### 3.4. METALLOGRAPHIC EXAMINATION

As a result of analyses of dispersion of various compositions it was found the following. Density of $UO_2$+Al composition with $UO_2$ particles in the form of spheres was 3.83 g/cm$^3$, and with particles in the form kernels was 3.94 g/cm$^3$. The matrix had fine-grain structure with the grain size of ~ 25 μm, uneven pores were observed in the matrix (Fig. 12).

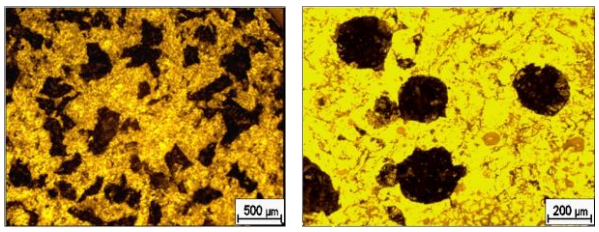


*a* *b*

*Fig. 12. Microstructure of $UO_2$+Al: a – $UO_2$ as kernels; b – $UO_2$ as spheres*

Pellet density made 96…98% of maximum calculated value.

### 3.5. CORROSION TESTING

Corrosion tests were performed using comparative rapid test method. The samples with composition $UO_2$+Al ($\rho_{pel}$ = 98.7% of FP) were tested in the form of pellets (∅7.6 mm, length of 8…10 mm) in autoclaves at the temperature of 50 °C in high purity water (deaerated water) under static condition. Test results are given in Fig. 13.

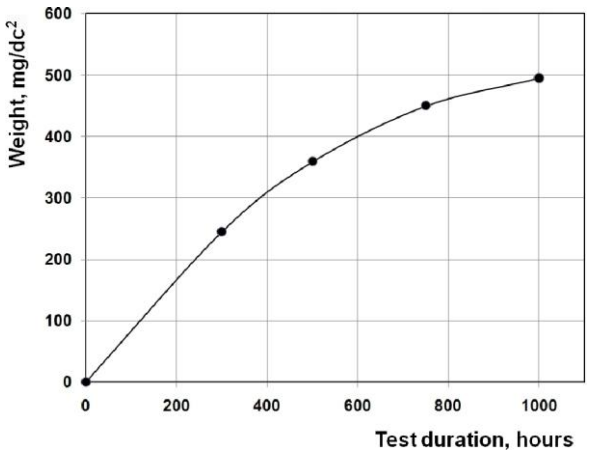


*Fig. 13. Weight gain – corrosion test duration relationship of pellets containing $UO_2$+Al at t =50 °C in high purity water under static conditions (SD ±5%)*

Also, testing of aluminium samples of different powder fractions and dispersion compositions with fuel particle simulators, which have demonstrated good corrosion resistance of the aluminium matrix, was executed [10]. Following on from the results of autoclave testing depicted in Fig. 13 and results obtained before [10], corrosion of samples occurs with weight gain. During the initial period of oxidation dramatic weight gain occurred almost linearly, which illustrated the intensive process of aluminium matrix oxidation and free penetration of corrosive medium into the sample.

With increasing time of exposure to static autoclaves corrosion rate decreased, meanwhile response of the curve of corrosion weight gain came close to the quadratic dependence, which was intrinsic to the process of the oxide film formation on the matrix surface. When examining the samples after corrosion tests it was observed that all samples retained integrity and initial geometry.

## CONCLUSIONS

1. Designs of fuel assemblies TVS-XD with dispersion compositions based on uranium dioxide dispersed in aluminium matrix were developed.

2. The process flow sheet of producing dispersion composition pellets, as well as fuel element and fuel rod assembly models are presented.

3. The dependence of temperature distribution over the cross section of fuel elements and maximum temperature values in pellet centres were determined. For TVS-XD1 и TVS-XD2 they are equal to ~ 95 and ~ 70 °C for the SCA, and ~ 315 and ~ 155 °C for the VVR-M, respectively.

4. In relation to reactor VVR-M, TVS-XD2 structure is more preferable since it has lower thermal load on fuel elements in comparison with TVS-XD1.

5. The design of dispersion fuel elements TVS-XD ensures non-exceedance of the established criteria of safe operation in the SCA and VVR-M according to the temperature of fuel composition and the chosen design.

## REFERENCES

1. Utility model patent No. 103259. *A fuel assembly for research reactors* / N.N. Belash, A.V. Kushtym, V.S. Krasnorutskiy, N.A. Lavrentiev. Publ. on 10.12.2015.

2. V.S. Krasnorutskiy, N.N. Belash, A.V. Kushtym, V.V. Zigunov. *A fuel assembly for nuclear research installation*. Application for an invention, Reg. No. a201608222 as of 25.07.2016.

3. Patent for invention No. 112268. *A method for obtaining dispersion fissible fuel* / N.N. Belash, A.V. Kushtym, V.V. Zigunov, V.S. Krasnorutskiy. Publ. on 10.08.2016.

4. A.V. Ostapov, A.V. Kushtym, I.A. Chernov. A modification of models by TRANSURANUS code for temperature evaluation in fuel elements containing dispersion fuel // *Proceedings of the School for young researchers in nuclear physics and energy*, Alushta, 2013.

5. Fissible fuel for research installations. *NCCP Catalogue of Products.*

6. Fuel assemblies VVER-M2. *Catalogue description*. NCCP, 2007.

7. V.A. Tsykanov. *Fuel elements for research reactors*. Dimitrovgrad: SSC RF RIAR, 2001, 249 p.

8. A.G. Samoilov, A.I. Kashtanov, V.S. Volkov. *Dispersion fuel rod assemblies*. M.: "Energoizdat", 1982, v. 1, 2.

9. V.N. Antsyferov, G.V. Bobrov, L.K. Druzhinin, S.S. Kiparisov, V.I. Kostikov, A.V. Krupin, V.V. Kudinov, G.A. Libenson, B.S. Mitin, O.V. Roman. *Powder metallurgy and sprayed-on coatings*. M.: «Metallurgiya», 1987, 792 p.

10. A.V. Kushtym, N.N. Belash, I.A. Chernov, V.M. Evseev, V.V. Zigunov, R.A. Rud, E.A. Slabospitskaya, V.A. Zuyok. The development of dispersion fuel with aluminium matrix for research reactors: *Book of reports of the 4th International Conference «Improving safety and efficiency in nuclear power generation industry»*. Odessa, SPC "Energoatom", 2016, N 2, p. 71-82.

*Article received 23.11.2016*

## ТОПЛИВО ДИСПЕРСИОННОГО ТИПА ДЛЯ ИССЛЕДОВАТЕЛЬСКИХ ЯДЕРНЫХ УСТАНОВОК

***А.В. Куштым, Н.Н. Белаш, В.В. Зигунов, Е.А. Слабоспицкая, В.А. Зуек***

Представлены конструкции и схемы изготовления стержневых твэлов и сборок ТВС-ХД с дисперсионной композицией $UO_2$+Al. Приведены результаты теплового расчета твэлов применительно к харьковской подкритической установке и киевскому исследовательскому реактору ВВР-М, их сравнительные характеристики, результаты металлографических исследований и коррозионных испытаний топливных таблеток.

## ПАЛИВО ДИСПЕРСІЙНОГО ТИПУ ДЛЯ ДОСЛІДНИЦЬКИХ ЯДЕРНИХ УСТАНОВОК

***А.В. Куштим, М.М. Бєлаш, В.В. Зігунов, О.О. Слабоспицька, В.А. Зуйок***

Представлені конструкції і схеми виготовлення стрижневих твелів і складання ТВЗ-ХД з дисперсійною композицією $UO_2$+Al. Наведено результати теплового розрахунку твелів стосовно харківської підкритичної установки та київського реактора ВВР-М, їхні порівняльні характеристики, результати металографічних досліджень та корозійних випробувань паливних таблеток.